Mechanism of How Salt-Gradient-Induced Charges Affect the Translocation of DNA Molecules through a Nanopore

Yuhui He,[†] Makusu Tsutsui,[†] Ralph H. Scheicher,[‡] Chun Fan,[§] Masateru Taniguchi,[†*] and Tomoji Kawai[†]
[†]The Institute of Scientific and Industrial Research, Osaka University, Osaka, Japan; [‡]Condensed Matter Theory Group, Department of Physics and Astronomy, Uppsala University, Uppsala, Sweden; and [§]Computer Center of Peking University, Peking University, Beijing, China

ABSTRACT Experiments using nanopores demonstrated that a salt gradient enhances the capture rate of DNA and reduces its translocation speed. These two effects can help to enable electrical DNA sequencing with nanopores. Here, we provide a quantitative theoretical evaluation that shows the positive net charges, which accumulate around the pore entrance due to the salt gradient, are responsible for the two observed effects: they reinforce the electric capture field, resulting in promoted molecule capture rate; and they induce cationic electroosmotic flow through the nanopore, thus significantly retarding the motion of the anionic DNA through the nanopore. Our multiphysical simulation results show that, during the polymer trapping stage, the former effect plays the major role, thus resulting in promoted DNA capture rate, while during the nanopore-penetrating stage the latter effect dominates and consequently reduces the DNA translocation speed significantly. Quantitative agreement with experimental results has been reached by further taking nanopore wall surface charges into account.

INTRODUCTION

Advances in fabrication methods of nanopores and nanochannels (1–6) have allowed for electrokinetic motion of biomolecules in nanofluidic systems to be investigated, and have invoked great interest in potential applications as electrical genome-sequencing devices (7–10). To reach the goal of decoding an entire human genome within hours and at a cost of less than US$1000, researchers have been striving to enhance both the rate at which DNA is captured by the nanopore and the dwell time of the DNA molecule inside the pore (11–13): an improved capture rate will result in higher throughput, while the prolonged translocation time addresses another major challenge of substantially slowing down the DNA translocation speed so that each nucleotide could be interrogated multiple times electrically, thus sampling over different configurations. However, these goals seem difficult to achieve simultaneously.

Recently, Wanunu et al. (14) demonstrated that the existence of a salt gradient across the nanopore can increase the capture rate and reduce the translocation speed. The direction of influence in both these effects would be of substantial benefit for DNA sequencing, as stated above. However, the theoretical understanding of the physical mechanism behind the observed two effects remains in controversy: how could the force that assists trapping of DNA near the nanopore entrance also cause a drag force that retards the bDNA-permeating motion through the pore once the molecule had been captured? An osmotic flow (OF) model was proposed, making the assumption that there exists an ion-depletion water layer and that the triggered OF under the presence of a salt gradient could facilitate DNA trapping (15). Although showing quantitative agreement with the experimentally demonstrated capture enhancement, an immediate inference of this model is that a larger salt gradient would also result in a higher DNA translocation speed (and thus a lower translocation time) due to the larger OF. This finding is in direct conflict with the experimental observations of Wanunu et al. (14).

In this work, we show that it is, instead, the positive net charges around the pore entrance caused by the salt gradient that play the key role in these two seemingly incompatible effects. The charges reinforce both the electric capture field and the cationic electroosmotic flow (EOF) through the pore, though the former expedites DNA motion while the latter delays it. Our quantitative evaluation illustrates that, at the molecule-trapping stage, the electrophoretic motion overwhelms the advection with EOF and, consequently, the capture rate is enhanced. In the following translocation stage, the salt-gradient-enhanced EOF would then significantly slow down DNA sliding within the pore. In other words, during the two subsequent processes, two mechanisms are responsible for the observed phenomenon, respectively, although they originate from the same source: the excessive cations accumulated near the pore mouth due to the salt gradient across the pore.

METHOD

Analytic E_z under salt gradient

Below we derive an analytical expression for z-component electrical field E_z in the open-pore system. We assume a roughly linear drop of salt concentration along nanopore axis (15):

$$C(z) = \frac{C_c - C_t}{L} z + \frac{C_c + C_t}{2},$$
$$C\left(-\frac{L}{2}\right) = C_t, \quad (1)$$
$$C\left(\frac{L}{2}\right) = C_c.$$

Submitted May 8, 2013, and accepted for publication May 20, 2013.

*Correspondence: taniguti@sanken.osaka-u.ac.jp

Editor: Hagan Bayley.

0006-3495/13/08/0776/7 $2.00

http://dx.doi.org/10.1016/j.bpj.2013.05.065

The above assumption is valid for a nanopore with a large pore aspect ratio (14). The requirement of electrical current conservation along pore axis results in the following expression of $E_z(z)$:

$$E_z(z) = \frac{C_c}{\frac{C_c - C_t}{L} z + \frac{C_c + C_t}{2}} E_c, \quad (2)$$

where $E_c(t)$ is the z-component E-field at the pore entrance(exit). Thereby, the resistance of the nanopore is estimated as follows:

$$R_p = \frac{U_p}{I} = \frac{\int_{-L/2}^{L/2} dz E_z(z)}{eN_c u_c \pi D^2/4} = \frac{1}{\mu(C_t - C_c)e} \frac{4L}{\pi D^2} \ln\left(\frac{C_t}{C_c}\right). \quad (3)$$

On the other hand, resistances in the *cis* and *trans* chambers are calculated with an access resistance model (16,17):

$$R_{c(t)} = \frac{\rho_{c(t)}}{2D} = \frac{1}{\mu C_{c(t)} e 2D}. \quad (4)$$

The total applied voltage across the pore is the sum of drops in the nanopore and the *cis* and *trans* chambers:

$$U_z = \left(\int_{-\infty}^{-L/2} dz + \int_{-L/2}^{L/2} dz + \int_{L/2}^{\infty} dz \right) E_z(z). \quad (5)$$

In this way, we arrive at the expression for $E_z(z)$ in the *cis* chamber for DNA capture,

$$E_z(z) = E_c \frac{D^2}{8\left(z - \frac{L}{2}\right)^2}, \quad (6)$$

where

$$E_c = \frac{U_z}{\frac{\pi D}{8}\left(1 + \frac{C_c}{C_t}\right) + L\frac{C_c}{C_t - C_c}\ln\left(\frac{C_t}{C_c}\right)}.$$

The above expression shows a nice agreement with the numerical results derived by multiphysical modeling and simulation.

DISTRIBUTION OF NET CHARGES

The device architecture used in the salt-gradient across-nanopore experiments (14) is sketched in Fig. 1. A cylindrical nanopore with diameter D and length L penetrates the SiN membrane that separates two chambers, one with KCl salt concentration C_c (*cis* side) and the other with concentration C_t (*trans* side) and $C_t > C_c$. A cross-pore voltage is applied, giving rise to an electric field pointing from the *trans* chamber to the *cis* so that anionic double-stranded DNA molecules are electrophoretically driven through the pore from the *cis* to the *trans* side. At the capture stage, DNA molecules are outside of the nanopore (open-pore approximation); at the translocation stage, the DNA segments inside the pore are modeled as an ideal cylinder with radius a centered with and oriented parallel to the

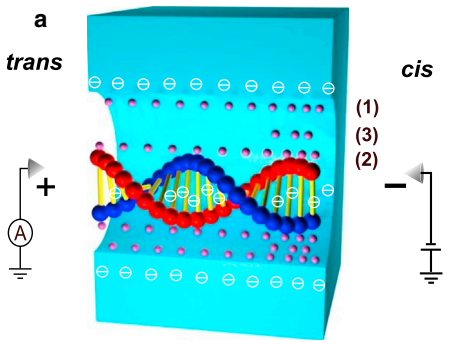

FIGURE 1 Schematic view of experimental setup: a nanopore is prepared in a membrane separating two chambers with different KCl salt concentrations (C_t in the *trans* and C_c in the *cis*) and an anionic DNA molecule is electrophoretically driven through the nanopore by applied cross-pore voltage U_z. Charges within EOF that retard DNA translocation consist of three parts: 1), those induced by the anionic DNA surface; 2), those induced by the negatively charged SiN pore wall surface; and 3), the excessive K^+ ions around the pore mouth rendered by salt gradient. (*Pink spheres*) Net charges in the solution, i.e., K^+ ions; (*open symbols*) fixed charges on SiN wall and DNA.

nanopore axis (18,19). The electrical double layers (EDLs) induced by the anionic polynucleotide passing through and by surface charges on the SiN pore wall are marked by Eqs. 7 and 8, respectively, for the following analysis of EOF.

The distributions of physical quantities in the open pore system were calculated by coupled solving of electrostatic, hydrodynamical, and ion transport equations (20–22):

$$\nabla \cdot \vec{E} = \nabla^2 U = -\frac{\rho_e}{\epsilon_f} = -\frac{e\sum_i z_i n_i}{\epsilon_f}, \quad (7)$$

$$-\nabla p + \mu \nabla^2 \vec{v} + e\sum_i z_i n_i \vec{E} = 0, \quad (8)$$

$$\nabla \cdot \vec{N}_i = \nabla \cdot (n_i \vec{v} - D_i \nabla n_i - \mu_i n_i \nabla U) = 0. \quad (9)$$

In the above equations, $\vec{E}$ is the electric field; U is the electrical potential; ρ_e is the net charge density; ϵ_f is permittivity of the fluid; n_i is the concentration of the ith ionic species; z_i is the valency of the ith ionic species; $\vec{v}$ is the velocity of the liquid; p is the hydrostatic pressure; μ is the fluid viscosity; $\vec{N}_i$ is the ionic flux density of the ith ionic species; D_i is the diffusivity; and μ_i is the electrophoretic mobility. The boundary conditions are as follows: for Eq. 1, the voltages at the ends of *cis* and *trans* chambers are $U_t = 0.3$ V and $U_c = 0$ V; for Eq. 2, open boundaries are used at the ends of *cis* and *trans* chambers as normal stress $f_z = 0$; for Eq. 3, the concentrations of KCl at the ends of *cis* and *trans* chambers are $C_t = 2$ M and $C_c = 0.1$ M. Simulations based on the above multiphysical model have shown nice agreements with previous experimental results (18,19,23).

Fig. 2 *a* plots the calculated net charge distribution defined as the local concentration difference between

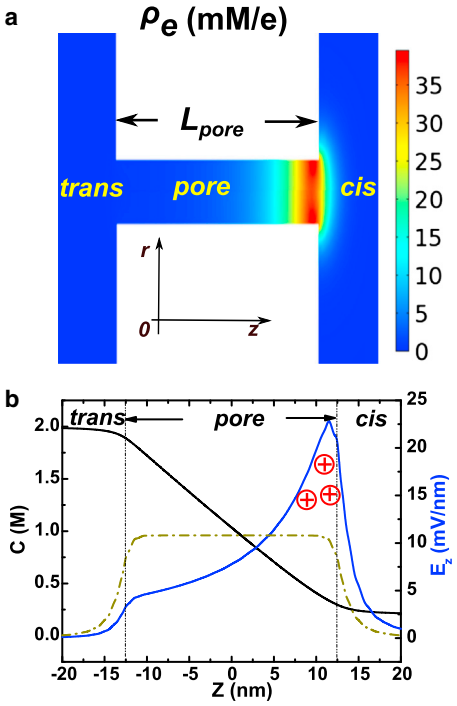

FIGURE 2 (*a*) Distribution of net charge density ρ_e in the nanopore axial-radial plane *z-r*. Here $C_t = 2$ M, $C_c = 0.1$ M, $D = 3.5$ nm, $L = 25$ nm, and $U_z = 300$ mV, just as in the experiments of Wanunu et al. (14). (*b*) Distribution of salt concentration C (*black line*) and *z*-component electric field E_z (*blue line*) along nanopore axial direction *z*. (*Red symbols*) The profile of $E_z(z)$ $E_z(z)$ demands positive net charges near the pore entrance. (*Dark-yellow line*) $E_z(z)$ under homogeneous salt concentration ($C_t = C_c = 1$ M).

cations and anions $\rho_e = C_K - C_{Cl}$ in the radial-axial *r-z* plane. More specifically, Fig. 2 *b* shows the salt concentration $C = C_K - C_{Cl}$ and *z*-component electric field E_z along the nanopore axis. This figure clearly demonstrates that there exists a peak in the E_z profile around the pore entrance, indicating positive net charges stacked there (according to Gauss's Law). Here we elucidate the physical origin of such a phenomenon through a brief analysis. The electrical current inside the open pore can be estimated as

$$I \approx \frac{e\pi D^2 \mu_K E_z(z) C(z)}{2},$$

where μ_K is the mobility of K^+ ions. The continuity of I along the pore axis leads to the requirement that the product of electrical field $E_z(z)$ and salt concentration $C(z)$ be independent of z within the pore. Because $C(z)$ decreases from C_t at the *trans* side to C_c at the *cis*, $E_z(z)$ should increase along that line from the pore exit to the entrance. On the other hand, once extending into the *cis* chamber, E_z decreases very rapidly. Therefore, there emerges a peak in the $E_z(z)$ profile around the pore entrance, which could only be achieved by excessive K^+ accumulating there. Compared to the electrical field in the case of homogeneous salt concentration (*dark-yellow line* in Fig. 2), these charges raise E_z near the pore mouth, and meanwhile cause larger cationic EOF through the pore.

DNA CAPTURE MOTION

Let us begin by studying the variation of the molecule capture rate for a given salt-gradient C_c/C_t. It has been proposed that DNA capture involves the following steps:

1. The polymer coils approach the pore from bulk in a diffusive manner;
2. Arriving at some critical distance to the pore entrance, the electric capture field takes effect;
3. The resulting drift motion from Step 2 overwhelms the pure diffusive motion; and
4. The polynucleotides have to overcome a conformational entropy barrier to get into the pore (14,24).

Thus, DNA motion is approximated as the sum of drift, diffusion, and advection near the pore mouth:

$$u_{\mathrm{DNA}} = u_{\mathrm{dr}} + u_{\mathrm{di}} + u_{\mathrm{ad}}. \tag{10}$$

The drift motion is estimated via the electrical capture field $\vec{E}$ in the *cis* chamber

$$u_{dr} = \mu_{\mathrm{DNA}} E,$$

where μ_{DNA} is the electrophoretic mobility of a DNA molecule in bulk solution. The magnitude of the diffusive motion u_{di} is orders-of-magnitude smaller than that of the drift motion within the capture range and thus can be safely neglected (15,22). The advection motion u_{ad} is the local fluid velocity determined by the EOF. Then, the distributions of electric field $\vec{E}$ and fluid velocity field $\vec{u}$ in the open-pore system were investigated by using the multiphysical model explained in the previous section. The calculated spatial distribution of u_{dr} and u_{ad} within the *cis* chamber are plotted in the inset of Fig. 3. It clearly demonstrates that the drift

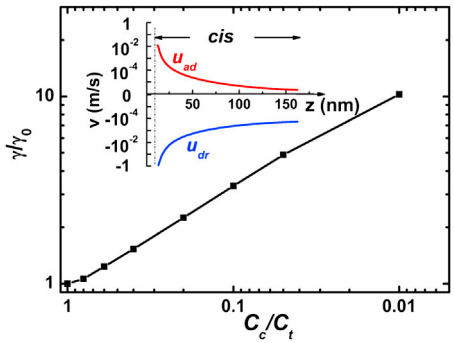

FIGURE 3 The DNA capture rate enhancement γ/γ_0 as a function of salt gradient C_c/Ct. All parameters are the same as in Fig. 2. (*Inset*) Plot of the DNA drift velocity u_{dr} by electric field and the advection u_{ad} by EOF within the *cis* reservoir. (*Vertical dash line*, *inset*) Location of pore mouth ($z = 12.5$ nm), while for $z > 12.5$ nm it is characterized as the *cis* reservoir.

motion is almost two orders-of-magnitude larger than the advection, i.e., the biopolymer capture is dominated by the electric-field trapping motion when a salt gradient exists. Regarding the physical mechanism, we speculate that drift motion is a direct consequence of the electrical field, while the advection is an indirect one; thus the former responds to the electrical field with much higher efficiency than the latter does. In our case, in the presence of an salt-gradient-enhanced electrical field around the pore entrance, DNA drift motion is raised straightforwardly; EOF is also boosted, and the advection motion acquired by the biopolymer is in the opposite direction to that of E-field driving. Much more dissipation should occur during the latter indirect accelerating process than that of drift motion. Therefore, at the DNA capture stage, $u_{\mathrm{DNA}} \approx u_{dr}$ when a salt gradient exists. With this in mind, we developed a simplified analytic model for evaluation of the E-field in the open-pore system (derivation details are provided in Method, above) and estimate the capture rate as follows (14,22):

$$\gamma \approx 2\pi z^2\, C_0\, \mu_{\mathrm{DNA}} E(z). \tag{11}$$

In the above expression, γ is the DNA capture rate; z is the distance of the DNA molecule from the open pore entrance; and C_0 is the far-field DNA molecule concentration. The above equation was derived based on the assumption that, around the nanopore entrance, $E(r) \sim r^{-2}$, which still stands under the cross-pore salt-gradient as seen in Method, above. The enhancement of the capture rate is then defined as γ/γ_0 (14), where γ_0 denotes the molecule capture rate for the case of a homogeneous salt concentration. This is an experimental observable and our calculation result is plotted in Fig. 3 as a function of salt gradient C_c/C_t. The results show agreement with the experimentally measured enhancement of the DNA capture rate (14). Thus, our model provides a potential explanation other than the osmotic flow model (15). That is, during the diffusion of DNA toward the nanopore entrance, the enhanced electric capture field in the presence of a salt gradient promotes the molecule trapping motion. As we are going to show in the following, our model would lead to another observation of reduced DNA translocating speed through the pore in the experiment, which could not be explained by osmotic flow model.

DNA TRANSLOCATION MOTION

After the capture into a SiN nanopore, the dominating dragging force of DNA translocation is the cationic EOF that moves in the opposite direction to the anionic DNA under the influence of an electrical driving field. (For extremely small diameter nanopores, DNA motion would be governed by direct interaction with the pore wall, which calls for molecular dynamical treatment with atomic resolution (25,26).) Mathematically, the velocity field of EOF within a nanopore is described by a steady-state Navier-Stokes equation for incompressible liquid (18). Assuming nanopore axial symmetry and fast equilibrium in the pore radial direction ($u\theta = 0$, $u_r = 0$) (18,20), we obtain the following equation in the cylinder coordinate:

$$\begin{aligned} \eta \frac{1}{r}\frac{\partial}{\partial r}\left(r\frac{\partial u_z}{\partial r}\right) &= \frac{\partial P}{\partial z} - E_z(z)\rho_e(r,z), \\ \frac{\partial u_z}{\partial z} &= 0, \end{aligned} \tag{12}$$

where u_z is the z-component fluid velocity; η is the fluid viscosity; P is the hydrodynamic pressure; E_z is the z-component electric field; and ρ_e is the charge density in the solution. After some mathematical treatment, Eq. 12 is reduced to an ordinary differential equation as below with no-slip boundary conditions:

$$\begin{aligned} \eta \frac{1}{r}\frac{d}{dr}\left(r\frac{du_z(r)}{dr}\right) &= \frac{-\int_{-L/2}^{L/2} dz E_z(z)\rho_e(r,z)}{L}, \\ u_z|_{r=R} &= 0, \\ u_z|_{r=a} &= u_{\mathrm{DNA}}. \end{aligned} \tag{13}$$

Here u_{DNA} is the steady-state translocation speed of the polynucleotide and a is the radius of the translocating polymer. The above equation indicates that ρ_e determines the velocity magnitude of EOF and thus the DNA speed, because it is proportional to the electrophoretic force exerted on EOF under electric driving field E_z. The value ρ_e consists of three parts within the pore as illustrated in Fig. 1:

1. Those induced by the anionic DNA molecule;
2. Those by the negatively charges on SiN wall; and
3. Excessive K^+ around the pore mouth caused by the salt gradient.

In this work, the effect of the last item is the central topic, while the other two have been studied elsewhere (18,19,23). Thus, we have made some separation approximation for Poisson equation

$$\nabla^2 \phi(\vec{r},z) = -\frac{\rho_e(\vec{r},z)}{\varepsilon_f}$$

to study the effect of item 3:

$$\begin{aligned} \phi(\vec{r},z) &= \phi_1(\vec{r}) + \phi_2(z), \\ \rho_e(\vec{r},z) &= \rho_1(\vec{r}) + \rho_2(z), \end{aligned} \tag{14}$$

where

$$\begin{aligned} \nabla_{\vec{r}}^2 \phi_1(\vec{r}) &= -\frac{\rho_1(\vec{r})}{\varepsilon_f}, \\ \frac{\partial^2 \phi_2(z)}{\partial z^2} &= -\frac{\partial}{\partial z}E_z(z) = -\frac{\rho_2(z)}{\varepsilon_f}. \end{aligned} \tag{15}$$

Accordingly, $\phi_1(\vec{r})$ is the potential built within the pore radial plane and $\phi_2(z)$ is the applied cross-pore potential. The validity of the above approximation will be shown in the last subsection. The value ϕ_1 is further calculated by assuming a Boltzmann distribution in the nanopore radial plane (20) and by combining it with the two boundary conditions near the charged pore wall surface and DNA molecule surface:

$$\begin{aligned} \nabla^2_{\vec{r}}\overline{\phi_1} &= \frac{\sinh\overline{\phi_1}}{\lambda_D^2}, \\ \left.\frac{\partial\overline{\phi_1}}{\partial r}\right|_{r=a} &= -\frac{e\lambda_{\mathrm{DNA}}}{2\pi a\varepsilon_f k_{\mathrm{B}}T}, \\ \left.\frac{\partial\overline{\phi_1}}{\partial r}\right|_{r=R} &= \frac{e\sigma_w}{\varepsilon_f k_{\mathrm{B}}T}, \end{aligned} \tag{16}$$

where $\overline{\phi_1} = e\phi_1/k_{\mathrm{B}}T$; $\lambda_D = \sqrt{\varepsilon_f k_{\mathrm{B}}T/2n_0e^2}$ is the Debye length; λ_{DNA} is the line-charge density of the double-stranded DNA molecule; and σ_w is the SiN wall surface charge density. In this manner, items 1 and 2 have been accounted for by $\rho_1(\vec{r})$, while item 3 has been accounted for by $\rho_2(z)$. Moreover, $\rho_2(z)$ can be estimated directly from the expression of $E_z(z)$, as shown by Eq. 2.

The steady-state DNA translocation is governed by the balanced force equation, written as follows:

$$\begin{aligned} \vec{F} &= f_{\mathrm{elec}} + f_{\mathrm{drag}} \\ &= \int_{-L/2}^{L/2} \left(E_z(z)\lambda_{\mathrm{DNA}} + \eta \frac{du_z(r)}{dr}\Big|_{r=a} 2\pi a \right) dz = 0. \end{aligned} \tag{17}$$

The terms of $E_z(z)$ and $u_z(r)$ in the above equation indicate that the electrostatic equation (Eq. 15) and hydrodynamic equation (Eq. 13) have been coupled. Therefore, a self-consistent calculation has to be performed to get quantities such as the DNA speed, fluid velocity field, and net charge distribution.

Previous studies showed that the negative nanopore wall surface charges were able to decrease the DNA translocation speed significantly through the induced cationic EOF within the pore (18,19,27). That is, contribution to the tuning of DNA velocity by item 2 shown in Fig. 1 is prominent. Nonetheless, in this work the regulation of DNA translocation by salt-gradient-induced EOF is the central topic, as depicted by item 3 of Fig. 1. Therefore, we put the discussion of DNA velocity under no influence of nanopore wall surface charges σ_w (see DNA Translocation Without Pore Wall Surface Charges) in the Supporting Material. Mathematically, it is done by manually setting $\sigma_w = 0$ in Eq. 16 and then solving those coupled equations. In this way, the variation of polymer motion by salt-gradient effect is singled out and the results shown in Fig. S1, Fig. S2, and Fig. S3 in the Supporting Material can be made in comparison with the following discussion under the influence of σ_w.

Fig. 4 *a* shows the calculated two-dimensional charge distribution in the nanopore axial-radial plane where the segments of translocating DNA inside the nanopore are approximated as a cylinder along nanopore axis. There are electrical double layers (EDLs) surrounding the surface of DNA ($r = 1$ nm) and that of the nanopore wall ($r = 4$ nm). It is intriguing to see that the two EDLs are thicker near the *trans* chamber side, while thinner around the *cis* side. This is attributed to the decreasing Debye length under larger salt concentration: $\lambda_D \sim 1/\sqrt{C}$. Also, ρ_e within the EDLs is approximately thousands of mM/e. Comparatively the charge distribution in the open nanopore neglecting wall surface charges is plotted in Fig. 4 *b*. In other words, Fig. 4 *a* shows the local concentration difference between cations and anions caused by three sources: 1), the anionic DNA molecule, 2), the negatively charged nanopore wall surface, and 3), the salt gradient; Fig. 4 *b* shows only the salt gradient. The value ρ_e in the latter case is approximately several mM/e, as seen in the figure. Because salt gradient effect is much smaller than that of pore wall surface charges, our separation approximation shown in Eq. 14 is valid in the sense that ϕ_2 can be viewed as a first-order perturbation term.

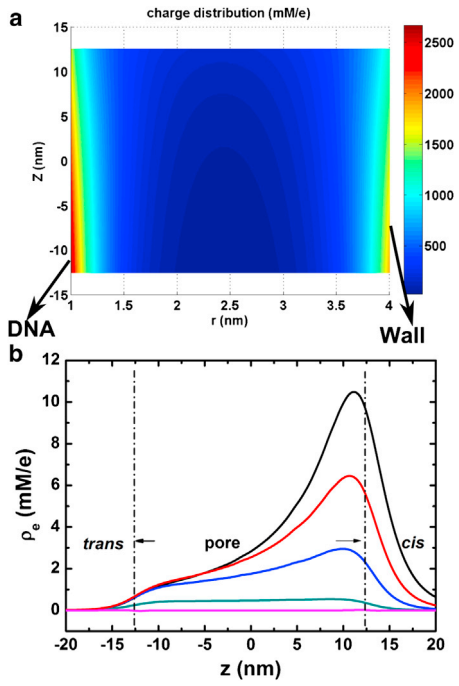

FIGURE 4 (*a*) Two-dimensional charge distribution with DNA inside the nanopore. Pore diameter $D = 8$ nm, and pore length $L = 25$ nm. The pore wall surface charge density $\sigma_w = -49$ C/m^2. (*b*) The calculated net charge density $\rho_e(z)$ along the nanopore axial direction when σ_w is manually set to be 0. Here C_t is fixed at 1 M, while C_c is tuned from 1 M (*magenta line*), to 0.8 M (*olive line*), to 0.4 M (*blue line*), to 0.2 M (*red line*), and finally to 0.1 M (*black line*).

The calculated fluid velocity $u_z(r)$ along nanopore radial direction is shown in Fig. 5. We remind the reader that $u_z|_{r=4\text{ nm}}$ is zero while $u_z|_{r=1\text{ nm}}$ is the DNA translocation speed due to the nonslip boundary conditions at the pore wall surface and at the DNA surface, respectively. The figure demonstrates that the overall liquid velocity is positive, indicating flow from *trans* ($z<0$) to *cis* chamber ($z>0$). Also, the larger the salt gradient ($C_c/C_t \to 0$), the smaller the DNA translocation speed, as shown in the inset of Fig. 5. The former effect of overall liquid flow direction is caused by the positive net charges accumulated in the nanopore and by the imposed electrical driving field pointing from *trans* to *cis* chamber. The latter effect, the stronger retarding of DNA motion under larger salt-gradient, is just what has been observed in the experiments. By comparing Fig. 5 with Fig. S2, we conclude that it is necessary to take the nanopore wall surface charges into consideration to achieve a quantitative match between the theoretical estimation of salt-gradient-modulated DNA translocation speed and the experimental report. Otherwise, neither the order of the calculated DNA speed, nor its variation trend with the imposed salt gradient, agrees with the experimental one.

The above conclusion is further demonstrated by comparing the inset of Fig. 6, where DNA translocation velocity u_{DNA} under homogeneous salt concentration (σ_w has been considered) is plotted, with Fig. S1, where the velocity of EOF caused merely by salt-gradient in the open pore is plotted. Without salt gradient, DNA speed is approximately several tens of μm/ms, while velocity of salt-gradient-generated EOF is also tens of μm/ms. They are of the same order, although in opposite directions. The fact indicates that, by imposing the salt gradient, the induced EOF would significantly retard the DNA translocation motion within the pore.

For the convenience of comparing with experimental observations, we define the enhancement of translocation time as $\tau/\tau_{\overline{C}}$, where τ is the translocation time under salt gradient while $\tau_{\overline{C}}$ is that under the associated homogeneous

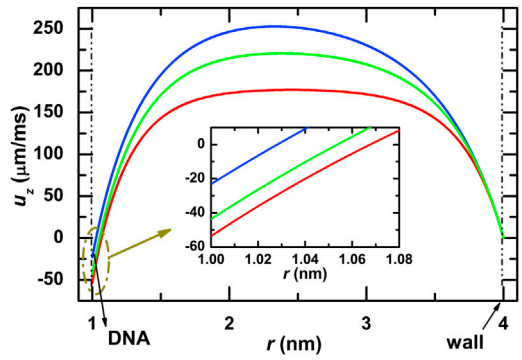

FIGURE 5 Fluid velocity $u_z(r)$ along nanopore radial direction under various salt gradients $C_c/Ct = 0.2$ (*blue line*), 0.5 (*green line*), and 1.0 (*red line*). Here C_t is fixed at 1 M, and the pore wall surface charge density is $\sigma_w = -49$ C/m^2.

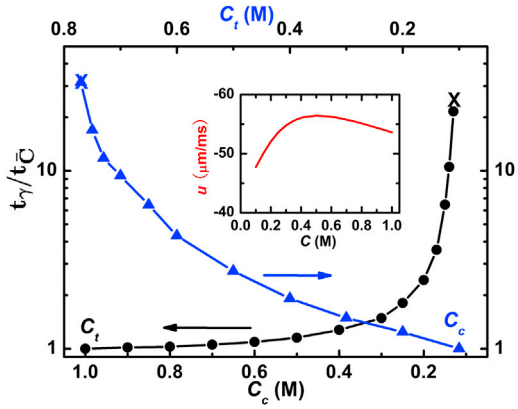

FIGURE 6 The enhancement of DNA translocation time $\tau/\tau_{\overline{C}}$, where τ is the translocation time under salt gradient and $\tau_{\overline{C}}$ is that within homogeneous salt solution, as a function of salt gradient C_c/Ct. Here $\overline{C} = (C_c + C_t)/2$. For the bottom-left coordinate, C_t is kept at 1 M while C_c is tuned from 1 to 0.1 M; for the top-right coordinate, C_c is kept at 0.1 M while C_t is tuned from 0.1 to 0.8 M. (*Inset*) DNA speed as a function of homogeneous salt concentration.

salt concentration $\overline{C} = (C_t + C_c)/2$. The value $\tau/\tau_{\overline{C}}$ can be examined by the experiments, and its dependence on the salt gradient is plotted in Fig. 6. For the bottom-left axes, we keep the salt concentration C_t invariant in the *trans* chamber while tuning C_c in *cis* chamber (thus, a smaller C_c corresponding to a larger salt gradient). For the upper-right axes C_c is constant and C_t is tuned (thus, a larger C_t corresponding to a larger salt gradient). This figure demonstrates that molecule translocation time keeps increasing with increasing salt gradient, and eventually, as shown by the cross ($\times$) symbols, also indicates that at sufficiently large salt gradient, the translocation time diverges to infinity. The above variation trend of DNA motion shown in the figure is consistent with experimental observation (14). It is worth pointing out that tuning the salt gradient would result in varying the average salt concentration $\overline{C}$ as well, which itself contributes to the altering of molecule speed (18,19,27). To assess this effect, DNA penetrating speed as a function of homogeneous salt concentration is further plotted in the inset of Fig. 6. The related variation magnitude is quite small compared to the overall tuning with the salt gradient. Thus, we conclude that the growth of the biopolymer translocation time is predominantly rendered by salt gradient-induced EOF.

CONCLUSIONS

In summary, we have studied the capture of DNA molecules and their penetrating process through a nanopore under the influence of a cross-pore salt gradient. We found that the positive net charges piled around the pore entrance are responsible for the experimentally observed increase of capture rate and translocation time. Our quantitative evaluation indicates that those charges promote, on the one hand, the

electric capture field at the DNA capture stage and, on the other hand, also increase the cationic electroosmotic flow, thus reducing the speed of DNA in the translocation stage. Moreover, as our calculation shows, the significance of nanopore wall surface charges on DNA translocation speed is demonstrated that only by taking these charges into account can quantitative agreement with experiment be obtained. The physical picture presented in this work gives a unified and consistent understanding for the experimental observations. Therefore, the model used in our work can be used to provide guidelines for optimizing DNA capture rate and translocation time by tuning the salt gradient.

SUPPORTING MATERIAL

Supporting analysis and six figures are available at http://www.biophysj.org/biophysj/supplemental/S0006-3495(13)00780-7.

This research is supported partially by the Japan Society for the Promotion of Science through its Funding Program for World-Leading Innovative R&D on Science and Technology. R.H.S. acknowledges financial support from the Swedish Foundation for International Cooperation in Research and Higher Education, and the Swedish Research Council (VR grant No. 621-2009-3628).

REFERENCES

1. Chen, P., T. Mitsui, …, D. Branton. 2004. Atomic layer deposition to fine-tune the surface properties and diameters of fabricated nanopores. *Nano Lett.* 4:1333–1337.
2. Dekker, C. 2007. Solid-state nanopores. *Nat. Nanotechnol.* 2:209–215.
3. Akeson, M., D. Branton, …, D. W. Deamer. 1999. Microsecond time-scale discrimination among polycytidylic acid, polyadenylic acid, and polyuridylic acid as homopolymers or as segments within single RNA molecules. *Biophys. J.* 77:3227–3233.
4. Chen, P., J. Gu, …, D. Branton. 2004. Probing single DNA molecule transport using fabricated nanopores. *Nano Lett.* 4:2293–2298.
5. Kasianowicz, J. J., E. Brandin, …, D. W. Deamer. 1996. Characterization of individual polynucleotide molecules using a membrane channel. *Proc. Natl. Acad. Sci. USA.* 93:13770–13773.
6. Meller, A., L. Nivon, …, D. Branton. 2000. Rapid nanopore discrimination between single polynucleotide molecules. *Proc. Natl. Acad. Sci. USA.* 97:1079–1084.
7. Meller, A., L. Nivon, and D. Branton. 2001. Voltage-driven DNA translocations through a nanopore. *Phys. Rev. Lett.* 86:3435–3438.
8. Deamer, D. W., and D. Branton. 2002. Characterization of nucleic acids by nanopore analysis. *Acc. Chem. Res.* 35:817–825.
9. Zwolak, M., and M. Di Ventra. 2005. Electronic signature of DNA nucleotides via transverse transport. *Nano Lett.* 5:421–424.
10. Lagerqvist, J., M. Zwolak, and M. Di Ventra. 2006. Fast DNA sequencing via transverse electronic transport. *Nano Lett.* 6:779–782.
11. Branton, D., D. W. Deamer, …, J. A. Schloss. 2008. The potential and challenges of nanopore sequencing. *Nat. Biotechnol.* 26:1146–1153.
12. Zwolak, M., and M. Di Ventra. 2008. Colloquium: physical approaches to DNA sequencing and detection. *Rev. Mod. Phys.* 80:141–165.
13. He, Y., M. Tsutsui, …, T. Kawai. 2012. DNA capture in nanopore for genome sequencing: challenges and opportunities. *J. Mater. Chem.* 22:13423–13427.
14. Wanunu, M., W. Morrison, …, A. Meller. 2010. Electrostatic focusing of unlabeled DNA into nanoscale pores using a salt gradient. *Nat. Nanotechnol.* 5:160–165.
15. Hatlo, M. M., D. Panja, and R. van Roij. 2011. Translocation of DNA molecules through nanopores with salt gradients: the role of osmotic flow. *Phys. Rev. Lett.* 107:068101.
16. Hall, J. E. 1975. Access resistance of a small circular pore. *J. Gen. Physiol.* 66:531–532.
17. Tsutsui, M., S. Hongo, …, T. Kawai. 2012. Single-nanoparticle detection using a low-aspect-ratio pore. *ACS Nano.* 6:3499–3505.
18. Ghosal, S. 2007. Effect of salt concentration on the electrophoretic speed of a polyelectrolyte through a nanopore. *Phys. Rev. Lett.* 98:238104.
19. He, Y., M. Tsutsui, …, T. Kawai. 2011. Controlling DNA translocation through gate modulation of nanopore wall surface charges. *ACS Nano.* 5:5509–5518.
20. Wong, C. T. A., and M. Muthukumar. 2007. Polymer capture by electro-osmotic flow of oppositely charged nanopores. *J. Chem. Phys.* 126:164903.
21. Muthukumar, M. 2010. Theory of capture rate in polymer translocation. *J. Chem. Phys.* 132:195101.
22. He, Y., M. Tsutsui, …, T. Kawai. 2011. Gate manipulation of DNA capture into nanopores. *ACS Nano.* 5:8391–8397.
23. Ai, Y., J. Liu, …, S. Qian. 2010. Field effect regulation of DNA translocation through a nanopore. *Anal. Chem.* 82:8217–8225.
24. Grosberg, A. Y., and Y. Rabin. 2010. DNA capture into a nanopore: interplay of diffusion and electrohydrodynamics. *J. Chem. Phys.* 133:165102.
25. Heng, J. B., A. Aksimentiev, …, G. Timp. 2005. Stretching DNA using the electric field in a synthetic nanopore. *Nano Lett.* 5:1883–1888.
26. Mirsaidov, U., J. Comer, …, G. Timp. 2010. Slowing the translocation of double-stranded DNA using a nanopore smaller than the double helix. *Nanotechnology.* 21:395501.
27. Smeets, R. M. M., U. F. Keyser, …, C. Dekker. 2006. Salt dependence of ion transport and DNA translocation through solid-state nanopores. *Nano Lett.* 6:89–95.